

ACCEPTED MANUSCRIPT

This is an early electronic version of an as-received manuscript that has been accepted for publication in the Journal of the Serbian Chemical Society but has not yet been subjected to the editing process and publishing procedure applied by the JSCS Editorial Office.

Please cite this article as D. Pardaeva, A. Tavman, M. Hacıoğlu, O. Şahin, M. Altun, and A. S. Birteksöz Tan, *J. Serb. Chem. Soc.* (2026) <https://doi.org/10.2298/JSC260217028P>

This “raw” version of the manuscript is being provided to the authors and readers for their technical service. It must be stressed that the manuscript still has to be subjected to copyediting, typesetting, English grammar and syntax corrections, professional editing and authors’ review of the galley proof before it is published in its final form. Please note that during these publishing processes, many errors may emerge which could affect the final content of the manuscript and all legal disclaimers applied according to the policies of the Journal.



J. Serb. Chem. Soc. **00(0)** 1-23 (2026)
JSCS-13789

Metal complexes with Schiff base and benzimidazolylphenol ligands with *tert*-butyl and methoxy groups: Structural characterization and biological evaluation

DILDORA PARDAEVA¹, AYDIN TAVMAN^{2,*}, MAYRAM HACIOGLU³, ONUR ŞAHİN⁴, MEHMET ALTUN⁵ AND AYŞE SEHER BIRTEKSÖZ TAN³

¹Istanbul University-Cerrahpaşa, Institute of Graduate Education, Department of Chemistry, 34320, Avcılar, Istanbul, Türkiye, ²Istanbul University-Cerrahpaşa, Faculty of Engineering, Department of Chemistry, Inorganic Chemistry Division, 34320, Avcılar, Istanbul, Türkiye, ³Istanbul University, Faculty of Pharmacy, Department of Pharmaceutical Microbiology, 34452, Beyazıt, Istanbul, Türkiye, ⁴Sinop University, Faculty of Health Sciences, Department of Occupational Health and Safety, 57000 Sinop, Türkiye, and ⁵Istanbul University-Cerrahpaşa, Faculty of Engineering, Department of Chemistry, Organic Chemistry Division, 34320, Avcılar, Istanbul, Türkiye.

(Received 17 February; revised 27 February; accepted 2 June 2026)

Abstract: Two chelating ligands bearing *tert*-butyl and methoxy groups, an ONO type Schiff base (**H₂L¹**) and a benzimidazolylphenol derivative (**HL²**), NO type ligand, and their complexes with CoCl₂, NiCl₂, CuCl₂, ZnCl₂ and K₂PdCl₄ (**1a** – **1e**, **2a** – **2e**) were synthesized and characterized. Various physicochemical and spectroscopic techniques were used to characterize the ligands. In addition, the crystal structure of **H₂L¹** was determined by X-ray diffraction spectroscopy. Keto-enol tautomerism is observed in **H₂L¹** according to spectral data. Elemental analysis, molar conductivity, magnetic moment, thermogravimetric analysis, FT-IR, fluorescence, UV-vis, and NMR (for diamagnetic complexes) spectroscopic techniques were utilized to characterize the complexes. Then, antibacterial, antifungal and antiviral activities of the compound were investigated. Antimicrobial activities of the compounds were tested toward six bacteria and three fungi. Some of the complexes exhibited higher activity towards some microorganisms than the ligands. **HL²** and its complexes were observed to show higher activity compared to **H₂L¹** and its complexes, especially against *S. aureus*, *S. epidermidis*, and *E. coli* bacteria, and the fungus *C. tropicalis*. It was found that **2a** has a potent activity against *S. aureus* and *E. coli*, **2b** against both Gram positive bacteria (*S. aureus* and *S. epidermidis*), and **2c** against *S. aureus*, *S. epidermidis* and *E. coli* compared to other complexes. Antiviral activity of the compounds was tested against Parainfluenza Type-2 virus. In terms of antiviral effect, **H₂L¹** showed higher activity than **HL²**; and the

* Corresponding author. E-mail: atavman@iuc.edu.tr
<https://doi.org/10.2298/JSC260217028P>

Co(II) and Cu(II) complexes of **HL**² had the highest activity among the compounds, with rates of 62 % and 64 %, respectively.

Keywords: chelating ligand; imine; transition metal complex; antimicrobial; antiviral.

INTRODUCTION

Imine compounds derived from *o*-aminophenols and salicylaldehydes are known as ONO type Schiff bases. Such ligands constitute a class of compounds of considerable interest because of their ability to form chelate structures, their variety of applications and many interesting properties.¹⁻⁴ They form strong chelate complexes due to their tridentate characteristics.⁵ ONO type Schiff bases are known to exhibit a wide range of biological effects such as antibacterial,^{6,7} antifungal,^{8,9} anticancer,¹⁰⁻¹³ antidiabetic¹⁴ activities. Due to these versatile characteristics, they have significant applications in both industry and biology.

A benzimidazole derivative containing a phenol group is called benzimidazolylphenol. Current and widespread research is being conducted on benzimidazolylphenols, and the results of these studies have the potential to be applied in many areas. In addition, since these compounds have strong fluorescent properties, many studies were published examining the photophysical properties of them and their complexes.¹⁵⁻¹⁷ We have also conducted various studies on many benzimidazolyl-phenol derivatives and some of their metal complexes, and we reported that these compounds have antimicrobial effects on some bacteria and fungi.¹⁸⁻²¹ For example, it was determined that 2-(5-bromo-1*H*-benzimidazol-2-yl)phenol compounds, especially those containing second and even third hydroxyl groups in the phenol ring, have both antioxidant and antibacterial effects that are considerably higher than others.²² Cl, Br and NO₂ groups in some 5-methoxy-2-(5-substituted-1*H*-benzimidazol-2-yl)-phenols were observed to increase the antimicrobial activity toward *S. aureus*, *E. faecalis* and *C. albicans*.²³

As is known, Cu(II) and Zn(II) ions are essential microelements in the human body having important roles in the human body such as modulate enzymes activities, catalytic and regulatory functions, oxidative-reductive processes, etc. Cobalt(II), which is a part of vitamin B12, is also an essential metal ion. Various biological activities of some Ni(II) and Pd(II) complexes were also reported.^{24,25}

The aim of this study is to prepare a salicylic-based Schiff base and benzimidazolylphenol ligands (**H₂L**¹ and **HL**², respectively) containing *tert*-butyl and methoxy groups and their metal complexes with CoCl₂, NiCl₂, CuCl₂, ZnCl₂ and K₂PdCl₄, and to investigate their structural properties and some biological effects. In the context of biological activity, the antibacterial, antifungal, and antiviral activities of all compounds were investigated. **H₂L**¹ and its various complexes were reported.²⁶⁻³⁰ 3d/4f Coordination clusters as cooperative catalysts for diastereoselective Michael addition reactions of Zn₂Y₂ complexes was

investigated by Griffiths *et al.*²⁶ Ke *et al* studied structures and magnetic properties of heterometallic Zn₂Dy₂ tetranuclear clusters of it.^{27,28} Antimicrobial activities of Ni(II) and Ni(II)+Zn(II) complexes of **H₂L¹** were investigated by Zhao *et al.*²⁹ Crystallographic insights and biological potency against malaria and oxidative stress of organotin complexes of **H₂L¹** was investigated.³⁰ **HL²**, a derivative of benzimidazolylphenol, is commercially available but is being published here for the first time.³¹

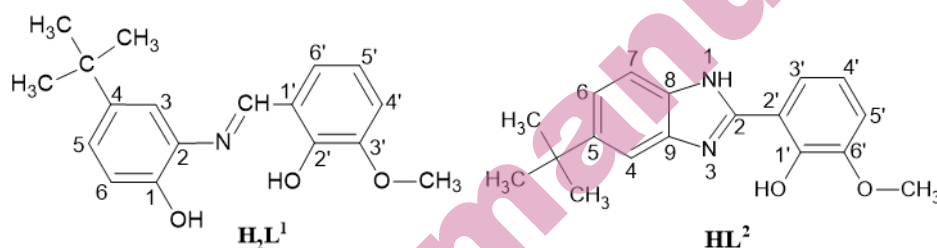


Fig. 1. Chemical structures of the ligands in the study.

EXPERIMENTAL

Chemistry and apparatus

All chemicals and solvents were of reagent grade and they were used without further purification.

The devices and techniques used are following: Elemental analysis: LECO combustion analyzer CHNS-932. Melting points: Buchi M-560 melting-point apparatus. Molar conductivity: WTW Cond315i conductivity meter (in DMF at 25 °C). Magnetic measurements: MK1 Sherwood Scientific apparatus (at room temperature by Gouy's method. Diamagnetic corrections were calculated using Pascal's constants). NMR spectroscopy: Varian Unity Inova 500 NMR spectrometer. FT-IR spectroscopy: Perkin Elmer Spectrum Two spectrometer with Attenuated Total Reflection (ATR) techniques, between 400 and 4000 cm⁻¹. The Electron Spray Ionization-Mass Spectroscopy (ESI-MS positive ion mode): Thermo Finnigan LCQ Advantage MAX LC/MS/MS (in MeOH). Thermogravimetric studies: TG-60WS Shimadzu, between 40 and 700 °C, with a heating rate of 10 °C/min and air flowing at the rate of 50 mL/min. UV-Visible spectra were performed on Shimadzu UV-1800 Spectrophotometer in EtOH. Fluorescence spectra: Shimadzu RF-5301 PC Spectrofluorophotometer ($c \approx 1 \times 10^{-4}$ mol/L in EtOH).

Synthesis of the ligands

4-*tert*-Butyl-2-{[(*E*)-(2-hydroxy-3-methoxyphenyl)methylidene]amino}phenol (**H₂L¹**): 3-Methoxysalicylaldehyde (0.78 g, 5 mmol) and 2-amino-4-*tert*-butylphenol (0.825 g, 5 mmol) were dissolved in EtOH (25 mL) and refluxed for 3 h. The crystals formed in the solution that was filtered and kept at room temperature. Red solid. Yield: 77 %. Decomposition point (Dec. p.): 138 °C. (+)ESI-MS (m/z): calculated for [C₁₈H₂₁NO₃]⁺ 299.4, observed 297.3 (90.6 %) ([C₁₈H₂₁NO₃ - 2H]⁺ and 300.4 for ([C₁₈H₂₁NO₃ + H]⁺ (64.1 %). Combustion analysis for C₁₈H₂₁NO₃: Calculated C 72.22, H 7.07, N 4.68; found C 72.41, H 7.11, N 4.60. FT-IR (ATR, cm⁻¹): 3509m,br ν (NH), 3054w ν (CH)_{ar.}, 2958m ν (CH)_{al.}, 1630m ν (C=N), 1619m ν (C=C),

1498m, 1455m, 1351m, 1289m, 1225m $\nu(\text{C}-\text{O})$, 1204m $\nu(\text{C}-\text{O})$, 1070s, 831m $\delta(\text{CH})_{\text{ar}}$, 740m, 623m, 572m, 465m, 425m. ^1H NMR (500 MHz, DMSO- d_6 , δ / ppm): 9.57 (s, 1H, OH1), 9.00 (s, 1H, N=CH), 7.36 (d, 1H, $J = 2.4$, H3), 7.21 (dd, 1H, $J_1 = 7.9$, $J_2 = 1.4$, H6'), 7.14 (dd, 1H, $J_1 = 8.5$, $J_2 = 2.4$, H5), 7.06 (dd, 1H, $J_1 = 8.0$, $J_2 = 1.4$, H4'), 6.89 (d, 1H, $J = 8.5$, H6), 6.84 (t, 1H, $J_1 = 7.9$, $J_2 = 7.9$, H5'), 3.81 (s, 3H, OCH₃), 1.28 (s, 9H, $-\text{C}(\text{CH}_3)_3$). ^{13}C NMR (125 MHz, DMSO- d_6 , δ / ppm): 161.6 (N=CH), 152.5 (C-OH(2')), 149.0 (C-OCH₃), 148.6 (C-OH(1')), 142.5 (C-C(CH₃)), 134.0 (C2), 125.2 (C5), 124.3 (C6'), 119.7 (C3), 118.2 (C6), 116.7 (C1'), 116.5 (C5'), 115.5 (C4'), 56.3 (OCH₃), 34.4 ($-\text{C}(\text{CH}_3)_3$), 31.8 ($-\text{C}(\text{CH}_3)_3$). UV-vis spectra (DMSO, λ_{max} / nm): 315m,br, 348m,br, 456w,br.

2-(5-*tert*-Butyl-1*H*-benzimidazol-2-yl)-6-methoxyphenol (**HL**²): A modified method developed by us utilizing two different methods available in the literature was applied for synthesis of **HL**².³²⁻³⁴ 3-Methoxysalicylaldehyde (0.78 g, 5 mmol), 4-*tert*-butylbenzene-1,2-diamine (0.82 g, 5 mmol) and 250 mg H₃BO₃ as catalyst were dissolved in DMF (25 mL) and then this mixture was refluxed for 3 h. After cooling to the room temperature, the reaction mixture was poured into water (250 mL) and then a precipitate was formed. It was filtered, dried and crystallized from ethanol after. Light yellow solid. Yield: 81 %. Dec.p.: 219 °C. (+)ESI-MS (m/z): calculated for [C₁₈H₂₀N₂O₂]⁺ 296.4, observed 297.3 (100 %) ([C₁₈H₂₀N₂O₂ - H]⁺ and 298.3 for ([C₁₈H₂₀N₂O₂ + 2H]⁺ (20.7 %). Combustion analysis for C₁₈H₂₀N₂O₂: Calculated C 72.95, H 6.80, N 9.45; found C 73.07, H 6.91, N 9.30. FT-IR (ATR, cm⁻¹): 3351m $\nu(\text{NH}+\text{OH})$, 3072w $\nu(\text{CH})_{\text{ar}}$, 2960m $\nu(\text{CH})_{\text{al}}$, 1619m $\nu(\text{C}=\text{N})$, 1604m $\nu(\text{C}=\text{C})$, 1576m, 1462m, 1364m, 1254s $\nu(\text{C}-\text{O})$, 1202m $\nu(\text{C}-\text{O})$, 1059m, 972m, 808m $\delta(\text{CH})_{\text{ar}}$, 785m, 732m, 655m, 557m, 511m, 457m, 425m. ^1H NMR (500 MHz, DMSO- d_6 , δ / ppm): 13.12 (s,br, 2H, NH+OH), 7.59 (dd, 1H, $J_1 = 8.0$, $J_2 = 1.3$, H6), 7.55 (s,br, 2H, H4+H6'), 7.36 (dd, 1H, $J_1 = 8.5$, $J_2 = 1.5$ Hz, H4'), 7.06 (dd, 1H, $J_1 = 8.0$, $J_2 = 1.2$, H7), 6.93 (t, 1H, $J_1 = 8.0$, $J_2 = 8.0$, H5'), 3.81 (s, 3H, OCH₃), 1.35 (s, 9H, $-\text{C}(\text{CH}_3)_3$). ^{13}C NMR (125 MHz, DMSO- d_6 , δ / ppm): 161.4 (C2), 152.7 (C-OCH₃), 149.6 (C-OH), 145.6 (C-C(CH₃)), 132.2 (C9), 131.3 (C8), 122.0 (C3'), 121.1 (C4'), 120.7 (C6), 120.1 (C2'), 117.1 (C7), 113.9 (C4), 109.3 (C5'), 56.2 (OCH₃), 34.5 ($-\text{C}(\text{CH}_3)_3$), 31.7 ($-\text{C}(\text{CH}_3)_3$). UV-vis spectra (DMSO, λ_{max} / nm): 304m, 316m, 330m,br, 382m,br. Fluorescence spectra (EtOH, $c = 1 \times 10^{-4}$ mol L⁻¹, λ_{max} / nm): 463m.

Preparation of the complexes

Appropriate metal salt solutions {1 mmol of CoCl₂·6H₂O, NiCl₂·6H₂O, ZnCl₂·6H₂O in 10 mL of ethylacetate; CuCl₂·2H₂O in 10 mL methanol, K₂PdCl₄ [was obtained by dissolving 1 mmol PdCl₂ (0.177 g) and 2 mmol KCl (0.15 g) in 10 mL MeOH+H₂O mixture (6:4, v/v)] were added gradually to the solutions of the ligands (1 mmol, i.e. ~300 mg of **HL**¹) in appropriate solvent (10 mL) and heated for 3 h under reflux. Cu(II) and Pd(II) salts gave immediately precipitates with the ligands. The other complex solutions were kept at room temperature, precipitates formed within a few days. The precipitates were filtered off, washed with distilled water and kept at room temperature to dry.

[Co(**L**¹)(H₂O)₂]-H₂O (**1a**): Brown solid. Yield: 67 %. Dec. p.: 167 °C. Combustion analysis for C₁₈H₂₅NO₆Co (FW: 410.33): Calculated C 52.69, H 6.14, N 3.41; found C 52.40, H 5.84, N 3.28. Magnetic moment, μ_{eff} : 4.06 μ_{B} . Λ_{M} (DMF, 25 °C, S m² mol⁻¹): 21.4. FT-IR (ATR, cm⁻¹): 3223m,br $\nu(\text{OH})$, 3062w,br $\nu(\text{CH})_{\text{ar}}$, 2957m $\nu(\text{CH})_{\text{al}}$, 1646m $\nu(\text{C}=\text{N})$, 1611m $\nu(\text{C}=\text{C})$, 1565m, 1490m, 1440m, 1362m, 1257s $\nu(\text{C}-\text{O})$, 1225m, 1096m, 1050m, 957m, 822m $\delta(\text{CH})_{\text{ar}}$, 723m, 684m $\nu(\text{N} \rightarrow \text{M})$, 541m $\nu(\text{O} \rightarrow \text{M})$, 495m, 452m. TGA (t / °C: weight loss, %): 50: 0.3; 75: 1.5; 100: 4.6 (1 mole of H₂O); 150: 7.8; 200: 9.5 (1 mole of H₂O); 250: 12.3; 300: 18.3; 350: 36.5; 400: 47.8; 450: 58.0; 500: 67.5; 550: 80.1; 600: 80.1; 650: 80.1; 700: 80.2 (Theoretical value of CoO: 18.3 %). UV-vis spectra (DMSO, λ_{max} / nm): 227w, 253m, 278m,br, 354m, 464m,br.

[Ni(L¹)(H₂O)₂] (**1b**): Greenish brown solid. Yield: 70 %. Dec. p.: 186 °C. Combustion analysis for C₁₈H₂₃NO₅Ni (FW: 392.07): Calculated C 55.14, H 5.91, N 3.57; found C 55.33, H 6.06, N 3.51. Magnetic moment, μ_{eff} : 2.04 μ_{B} . A_{M} (DMF, 25 °C, S m² mol⁻¹): 21.4. FT-IR (ATR, cm⁻¹): 3065w,br $\nu(\text{CH})_{\text{ar}}$, 2957m $\nu(\text{CH})_{\text{al}}$, 1633sh $\nu(\text{C}=\text{N})$, 1615m $\nu(\text{C}=\text{C})$, 1506m, 1440m, 1362m, 1245m $\nu(\text{C}-\text{O})$, 1222s, 1129m, 1078m, 975m, 820m $\delta(\text{CH})_{\text{ar}}$, 732s, 682m $\nu(\text{N}\rightarrow\text{M})$, 587m, 536m $\nu(\text{O}\rightarrow\text{M})$, 496m, 454m, 425m. TGA (t / °C: weight loss, %): 50: 0.2; 75: 0.3; 100: 0.4; 150: 3.1; 200: 12.3 (2 mole of H₂O); 250: 15.5; 300: 22.1; 350: 27.2; 400: 60.1; 450: 78.9; 500: 80.0; 550: 80.0; 600: 80.0; 650: 80.0; 700: 80.0 (Theoretical value of NiO: 19.1 %). UV-vis spectra (DMSO, λ_{max} / nm): 232w, 255m, 300m,br, 343m,br, 356sh, 440m,br.

[Cu(L¹)(H₂O)] (**1c**): Brown solid. Yield: 73 %. Dec. p.: 295 °C. Combustion analysis for C₁₈H₂₁NO₄Cu (FW: 378.9): Calculated C 57.69, H 4.36, N 2.64; found C 57.43, H 4.21, N 2.49. Magnetic moment, μ_{eff} : 1.72 μ_{B} . A_{M} (DMF, 25 °C, S m² mol⁻¹): 32.0. FT-IR (ATR, cm⁻¹): 3346m,br $\nu(\text{OH})$, 3080w,br $\nu(\text{CH})_{\text{ar}}$, 2962m $\nu(\text{CH})_{\text{al}}$, 1647m $\nu(\text{C}=\text{N})$, 1612m $\nu(\text{C}=\text{C})$, 1588m, 1506m, 1463m, 1351m, 1258m $\nu(\text{C}-\text{O})$, 1093m, 1027m, 821m $\delta(\text{CH})_{\text{ar}}$, 781m, 731m, 688m $\nu(\text{N}\rightarrow\text{M})$, 584m, 537m $\nu(\text{O}\rightarrow\text{M})$, 477m, 422m. TGA (t / °C: weight loss, %): 50: 0.1; 75: 0.4; 100: 0.6; 150: 4.4; 200: 5.0 (1 mole of H₂O); 250: 10.5; 300: 29.8; 350: 45.1; 400: 47.0; 450: 59.7; 500: 68.0; 550: 79.2; 600: 79.4; 650: 79.9; 700: 79.9 (Theoretical value of CuO: 21.0 %). UV-vis spectra (DMSO, λ_{max} / nm): 242w, 254m, 272m,br, 307sh, 363m,br, 478w,br.

[Zn(L¹)(H₂O)]·H₂O (**1d**): Dark yellow solid. Yield: 65 %. Dec. p.: 173 °C. Combustion analysis for C₁₈H₂₃NO₅Zn (FW: 398.8): Calculated C 49.79, H 5.34, N 3.23; found C 49.90, H 5.20, N 3.11. A_{M} (DMF, 25 °C, S m² mol⁻¹): 23.4. FT-IR (ATR, cm⁻¹): 3336m,br $\nu(\text{OH})$, 3211m,br, 3061w,br $\nu(\text{CH})_{\text{ar}}$, 2957m $\nu(\text{CH})_{\text{al}}$, 1637m $\nu(\text{C}=\text{N})$, 1615m $\nu(\text{C}=\text{C})$, 1506m, 1435m, 1363m, 1285m, 1234m $\nu(\text{C}-\text{O})$, 1195m $\nu(\text{C}-\text{O})$, 1022m, 875m, 819m $\delta(\text{CH})_{\text{ar}}$, 734m, 684m $\nu(\text{N}\rightarrow\text{M})$, 586m, 537m $\nu(\text{O}\rightarrow\text{M})$, 497m, 415m. ¹H NMR (500 MHz, DMSO-d₆, δ / ppm): 8.86 (s, 1H, N=CH), 7.50 (s,br, 1H, J = 2.4, H3), 7.19 (d, 1H, J = 7.1, H6'), 7.03 (s,br, 1H, H5), 6.88 (s,br, 1H, H4'), 6.78 (d,br, 1H, J = 6.8, H6), 6.38 (t, 1H, J_1 = 7.7, J_2 = 7.8, H5'), 3.75 (s, 3H, OCH₃), 1.27 (s, 9H, -C(CH₃)₃). ¹³C NMR (125 MHz, DMSO-d₆, δ / ppm): 164.8 (N=CH), 161.3 (C-OH₂), 152.7 (C-OCH₃), 144.8 (C-OH1'), 142.4 (C-C(CH₃)), 130.1 (C2), 127.3 (C5), 123.8 (C6'), 119.4 (C3), 117.1 (C6), 114.3 (C1'), 111.5 (C5'), 107.6 (C4'), 55.0 (OCH₃), 32.2 (-C(CH₃)₃), 29.5 (-C(CH₃)₃). TGA (t / °C: weight loss, %): 50: 1.1; 75: 2.5; 100: 4.6 (1 mole of H₂O); 150: 4.4; 200: 9.5 (1 mole of H₂O); 250: 12.2; 300: 23.1; 350: 29.5; 400: 33.0; 450: 63.0; 500: 78.6; 550: 78.8; 600: 78.9; 650: 79.0; 700: 79.0 (Theoretical value of ZnO: 20.4%). UV-vis spectra (DMSO, λ_{max} / nm): 228 w, 253 w, 279 m, 354 m,br, 464 m,br.

K[Pd(L¹)Cl]·H₂O (**1e**): Light brown solid. Yield: 77 %, Dec. p.: 265 °C. Combustion analysis for C₁₈H₂₁ClNO₄KPd (FW: 496.3): Calculated C 43.56, H 4.26, N 2.82; found C 43.70, H 4.11, N 2.68. A_{M} (DMF, 25 °C, S m² mol⁻¹): 83.2. FT-IR (ATR, cm⁻¹): 3036m,br $\nu(\text{CH})_{\text{ar}}$, 2958m $\nu(\text{CH})_{\text{al}}$, 1646m $\nu(\text{C}=\text{N})$, 1611m $\nu(\text{C}=\text{C})$, 1506m, 1456m, 1351m, 1289m, 1257s $\nu(\text{C}-\text{O})$, 1204m $\nu(\text{C}-\text{O})$, 1097m, 1024m, 965m, 912m, 826m $\delta(\text{CH})_{\text{ar}}$, 730m, 673m $\nu(\text{N}\rightarrow\text{M})$, 564m, 540m $\nu(\text{O}\rightarrow\text{M})$, 500m, 462m. ¹H-NMR (500 MHz, DMSO-d₆, δ / ppm): 8.64 (s, 1H, N=CH), 7.94 (d, 1H, J =3.0, H3), 7.43 (d, 1H, J =8.1 H6'), 7.30 (d, 1H, J =8.5, H5), 7.09 (d, 1H, J = 8.2, H4'), 7.02 (d, 1H, J = 8.6, H6), 6.72 (t, 1H, J_1 = 8.7, J_2 = 8.5, H5'), 3.72 (s, 3H, OCH₃), 1.30 (s, 9H, -C(CH₃)₃). ¹³C NMR (125 MHz, DMSO-d₆, δ / ppm): 174.3 (N=CH), 161.5 (C-OH₂), 148.4 (C-OCH₃), 146.9 (C-OH1'), 139.5 (C-C(CH₃)), 134.3 (C2), 126.3 (C5), 125.3 (C6'), 118.4 (C3), 118.3 (C6), 115.2 (C1'), 113.6 (C5'), 112.5 (C4'), 55.9 (OCH₃), 35.7 (-C(CH₃)₃), 32.1 (-C(CH₃)₃). TGA (t / °C: weight loss, %): 50: 0.7; 75: 2.0; 100: 3.7 (1 mole of H₂O); 150: 3.9; 200: 4.1; 250: 4.3; 300: 6.0; 350: 7.5; 400: 20.0; 450: 67.0; 500: 74.7; 550: 75.3; 600: 75.6;

650: 75.9; 700: 76.0 (Theoretical value of PdO: 24.6 %). UV-vis spectra (DMSO, λ_{\max} / nm): 233w, 255m, 309sh, 318m,br, 337sh, 430m,br, 451sh.

[Co(L²)Cl(H₂O)] (**2a**): Dark brown solid. Yield: 72 %. Dec. p.: 201 °C. Combustion analysis for C₁₈H₂₁ClN₂O₃Co (FW: 407.8): Calculated C 53.02, H 5.19, N 6.87; found C 54.10, H 5.00, N 6.72. Magnetic moment, μ_{eff} : 2.17 μ_{B} . A_{M} (DMF, 25 °C, S m² mol⁻¹): 35.4. FT-IR (ATR, cm⁻¹): 3198m,br $\nu(\text{OH})$, 3088m,br $\nu(\text{CH})_{\text{ar}}$, 2960m $\nu(\text{CH})_{\text{al}}$, 1606m $\nu(\text{C}=\text{N})$, 1573m $\nu(\text{C}=\text{C})$, 1463m, 1435m, 1361m, 1244s $\nu(\text{C}-\text{O})$, 1195m, 1060m, 981m, 813m $\delta(\text{CH})_{\text{ar}}$, 786m, 732s, 66m $\nu(\text{N}\rightarrow\text{M})$, 601m, 574m, 545m $\nu(\text{O}\rightarrow\text{M})$, 501m, 470m, 420m. TGA (t / °C: weight loss, %): 50: 0.1; 75: 0.2; 100: 0.4; 150: 3.1; 200: 5.2 (1 mole of H₂O); 250: 9.9; 300: 29.0; 350: 66.0; 400: 67.1; 450: 68.2; 500: 69.4; 550: 82.4; 600: 82.5; 650: 82.6; 700: 82.6 (Theoretical value of CoO: 18.4 %). UV-vis spectra (DMSO, λ_{\max} / nm): 240w, 253w, 307m,br, 320m,br, 334sh, 473w,br. Fluorescence spectra (EtOH, $c = 1 \times 10^{-4}$ mol L⁻¹, λ_{\max} / nm): 425sh, 451m,br.

[Ni(L²)Cl(H₂O)]·H₂O (**2b**): Light brown solid. Yield: 70 %. Dec. p.: 198 °C. Combustion analysis for C₁₈H₂₃ClN₂O₄Ni (FW: 425.5): Calculated C 50.81, H 5.45, N 6.58; found C 50.90, H 5.51, N 6.43. Magnetic moment, μ_{eff} : 2.05 μ_{B} . A_{M} (DMF, 25 °C, S m² mol⁻¹): 38.8. FT-IR (ATR, cm⁻¹): 3373m,br $\nu(\text{OH})$, 3228m,br, 3070m,br $\nu(\text{CH})_{\text{ar}}$, 2962m $\nu(\text{CH})_{\text{al}}$, 2872m, 1611m $\nu(\text{C}=\text{N})$, 1598m $\nu(\text{C}=\text{C})$, 1545m, 1440m, 1362m, 1249m $\nu(\text{C}-\text{O})$, 1198m $\nu(\text{C}-\text{O})$, 1015m, 983m, 863m, 814m $\delta(\text{CH})_{\text{ar}}$, 731m, 671m $\nu(\text{N}\rightarrow\text{M})$, 581m, 540m $\nu(\text{O}\rightarrow\text{M})$, 457m, 420m. TGA (t / °C: weight loss, %): 50: 0.3; 75: 2.2; 100: 4.6 (1 mole of H₂O); 150: 7.8; 200: 9.0 (1 mole of H₂O); 250: 19.3; 300: 22.8; 350: 24.4; 400: 36.9; 450: 53.0; 500: 65.1; 550: 72.1; 600: 75.3; 650: 82.6; 700: 83.0 (Theoretical value of NiO: 17.5 %). UV-vis spectra (DMSO, λ_{\max} / nm): 241w, 253w, 309m,br, 357m,br, 373m,br, 461m,br. Fluorescence spectra (EtOH, $c = 1 \times 10^{-4}$ mol L⁻¹, λ_{\max} / nm): 399w, 478m.

[Cu(L²)Cl] (**2c**): Brown solid. Yield: 76 %. Dec. p.: 235 °C. Combustion analysis for C₁₈H₁₉ClN₂O₂Cu (FW: 394.4): Calculated C 54.82, H 4.86, N 7.10; found C 55.90, H 5.05, N 6.92. Magnetic moment, μ_{eff} : 1.01 μ_{B} . A_{M} (DMF, 25 °C, S m² mol⁻¹): 48.8. FT-IR (ATR, cm⁻¹): 3215m,br $\nu(\text{OH})$, 3057w,br $\nu(\text{CH})_{\text{ar}}$, 2962m $\nu(\text{CH})_{\text{al}}$, 1608m $\nu(\text{C}=\text{N})$, 1589m $\nu(\text{C}=\text{C})$, 1543m, 1485m, 1384m, 1242s $\nu(\text{C}-\text{O})$, 1199m $\nu(\text{C}-\text{O})$, 1062m, 981m, 815m $\delta(\text{CH})_{\text{ar}}$, 786m, 732s, 667m $\nu(\text{N}\rightarrow\text{M})$, 576m, 543m $\nu(\text{O}\rightarrow\text{M})$, 470m, 418m. TGA (t / °C: weight loss, %): 50: 0.2; 75: 0.3; 100: 0.4; 150: 0.5; 200: 1.6; 250: 4.2; 300: 6.4; 350: 13.4; 400: 26.5; 450: 43.0; 500: 65.0; 550: 76.0; 600: 78.1; 650: 80.0; 700: 81.0 (Theoretical value of CuO: 20.2 %). UV-vis spectra (DMSO, λ_{\max} / nm): 243w, 255m, 297sh, 307m, 321m, 335m,br, 371sh, 433m,br. Fluorescence spectra (EtOH, $c = 1 \times 10^{-4}$ mol L⁻¹, λ_{\max} / nm): 404w,br, 461sh.

[Zn(L²)Cl(H₂O)]·H₂O (**2d**): Dark yellow solid. Yield: 65 %, Dec. p.: 229 °C. Combustion analysis for C₁₈H₂₃ClN₂O₄Zn (FW: 432.3): Calculated C 50.02, H 5.36, N 6.48; found C 50.30, H 5.44, N 6.34. A_{M} (DMF, 25 °C, S m² mol⁻¹): 38.6. FT-IR (ATR, cm⁻¹): 3406m,br $\nu(\text{OH})$, 3215m,br $\nu(\text{NH})$, 3059w,br $\nu(\text{CH})_{\text{ar}}$, 2962m $\nu(\text{CH})_{\text{al}}$, 1614m $\nu(\text{C}=\text{N})$, 1591m $\nu(\text{C}=\text{C})$, 1554m, 1467m, 1386m, 1249s $\nu(\text{C}-\text{O})$, 1199m $\nu(\text{C}-\text{O})$, 1109m, 1078m, 975m, 852m, 825m $\delta(\text{CH})_{\text{ar}}$, 732s, 669m $\nu(\text{N}\rightarrow\text{M})$, 601m, 543m $\nu(\text{O}\rightarrow\text{M})$, 439m, 410m. ¹H NMR (500 MHz, DMSO-d₆, δ / ppm): 13.64 (s,br, 1H, NH), 7.65 (dd,br, 1H, $J_1 = 8.6$, $J_2 = 1.7$, H6), 7.37 (d,br, 2H, $J = 8.9$, H4+H6'), 7.05 (s,br, 1H, H4'), 6.95 (d,br, 1H, $J = 7.9$, H7), 6.89 (t,br, 1H, $J_1 = 8.0$, $J_2 = 8.1$, H5'), 3.82 (s, 3H, OCH₃), 1.36 (s, 9H, -C(CH₃)₃). ¹³C NMR (125 MHz, DMSO-d₆, δ / ppm): 167.9 (C2), 159.0 (C-OCH₃), 131.9, 104.7, 54.2 (OCH₃), 32.8 (-C(CH₃)₃). TGA (t / °C: weight loss, %): 50: 1.9; 75: 4.1; 100: 4.3 (1 mole of H₂O); 150: 8.4; 200: 9.0 (1 mole of H₂O); 250: 21.7; 300: 34.3; 350: 75.6; 400: 80.9; 450: 81.1; 500: 81.5; 550: 81.6; 600: 81.8; 650: 82.0; 700: 82.1 (Theoretical value of ZnO: 18.8 %). UV-vis spectra (DMSO, λ_{\max} / nm): 237w, 254w,

296sh, 304m, 332sh, 354sh. Fluorescence spectra (EtOH, $c = 1 \times 10^{-4}$ mol L⁻¹, λ_{\max} / nm): 424m,br.

[Pd(L²)Cl(H₂O)] (**2e**): Light brown solid. Yield: 77%, Dec. p.: 265. Combustion analysis for C₁₈H₂₁ClN₂O₃Pd (FW: 455.2): Calculated C 47.49, H 4.65, N 6.15; found C 47.12, H 4.63, N 5.90. A_M (DMF, 25 °C, S m² mol⁻¹): 49.6. FT-IR (ATR, cm⁻¹): 3293m,br ν (OH), 3197m ν (NH), 3058w,br ν (CH)_{ar}, 2958m ν (CH)_{al}, 2866m, 1602m ν (C=N), 1592m ν (C=C), 1561m, 1492m, 1436m, 1364m, 1242s ν (C-O), 1182m ν (C-O), 1075m, 981m, 812m δ (CH)_{ar}, 733m, 669m ν (N→M), 599m, 543m ν (O→M), 465m, 441m. ¹H NMR (500 MHz, DMSO-d₆, δ / ppm): 13.22 (*s,br*, 1H, NH), 8.02 (*d*, 1H, $J = 9.1$, H6), 7.61 (*d,br*, 1H, $J = 2.8$, H4), 7.39 (*d,br*, 1H, $J = 8.8$, H6'), 7.30 (*dd*, 1H, $J_1 = 8.4$, $J_2 = 1.8$, H4'), 7.23 (*dd*, 1H, $J_1 = 8.6$, $J_2 = 1.6$, H7), 6.96 (*t*, 1H, $J_1 = 8.3$, $J_2 = 7.9$, H5'), 3.84 (*s*, 3H, OCH₃), 1.39 (*s*, 9H, -C(CH₃)₃). ¹³C NMR (125 MHz, DMSO-d₆, δ / ppm): 170.8 (C2), 166.2 (C-OCH₃), 159.8 (C-OH), 158.0 (C-C(CH₃)₃), 140.4, 139.3, 132.5, 119.0, 116.1, 56.2 (OCH₃), 33.2 (-C(CH₃)₃). TGA (t / °C: weight loss, %): 50: 0.2; 75: 0.5; 100: 0.6; 150: 3.3; 200: 5.1 (1 mole of H₂O); 250: 7.5; 300: 15.0; 350: 23.0; 400: 28.5; 450: 32.5; 500: 35.2; 550: 44.2; 600: 68.2; 650: 74.1; 700: 74.2 (Theoretical value of PdO: 26.8 %). UV-vis spectra (DMSO, λ_{\max} / nm): 233m, 255m, 308m,br, 321m,br, 335m,br, 458m,br. Fluorescence spectra (EtOH, $c = 1 \times 10^{-4}$ mol L⁻¹, λ_{\max} / nm): 393w, 472m,br.

Determination of antibacterial and antifungal activity

Antimicrobial activities of the compounds were investigated against standard ATCC strains of bacteria and fungi by the microbroth dilutions way according to the Clinical and Laboratory Standards Institute (CLSI) guidance.^{35,36} The antimicrobial activity procedure and the microorganisms used are the same as in our previous studies.^{8,9} The experiments were carried out in duplicate.

Antiviral activity assay

For Parainfluenza Type-2 virus (PIV-2), African green monkey kidney cell line (VERO, ATCC) was cultured in Dulbecco's modified Eagle's medium (Wisent, MULTICELL) supplemented with 10% fetal bovine serum (FBS; Sigma), 100 U/mL penicillin, and 100 μ g/mL streptomycin. The PIV-2 and cells were maintained at 37 °C under 5% CO₂ atmosphere. An experiment was conducted based on the plaque formation test for PIV-2 strain that grown on VERO cell culture.³⁷ VERO cells were infected with PIV-2 at 100 PFU per well, one of the wells was used as a control and the antiviral activities of the samples were tested in the other wells. The virus-infected control (Ribavirin) well was accepted as 100%, and the efficacy results were calculated as a percentage by comparing this control value. The concentration of the compounds is 10 mg/mL.

X-ray single crystal diffraction analysis

H₂L¹ was crystallized from EtOH. The red colored single crystals were obtained. Suitable crystals were selected for data collection which was performed on a Bruker-D8 QUEST diffractometer equipped with a graphite-monochromatic Mo-K α radiation at 296 K. The structure of **H₂L¹** was solved by direct methods using SHELXS-2013³⁸ and refined by full-matrix least-squares methods on F² using SHELXL-2013.³⁹ All non-hydrogen atoms were refined with anisotropic parameters. The H atoms of C atoms were located from different maps and then treated as riding atoms with C-H distance of 0.93 – 0.97 Å. The other H atoms were located in a difference map refined freely. The following procedures were implemented in our analysis: data collection: Bruker APEX2;⁴⁰ program used for molecular graphics were as follow: MERCURY programs;⁴¹ software used to prepare material for publication: WinGX.⁴² Details of data collection and crystal structure determinations are given in Table I. Crystallographic

data for the structural analysis are deposited with the Cambridge Crystallographic Data Centre, CCDC No. 2298000.

RESULTS AND DISCUSSION

Crystal structure of **H₂L¹**

Crystal data and structure refinement and hydrogen bond parameters related **H₂L¹** are given in Tables I and II, respectively. Selected bond distances and angles are given in Table S1. Molecular structure of **H₂L¹** is shown in Figure 2.

From the X-ray data, it appears that the keto structure is valid **H₂L¹** in solid state as in our previous studies.^{2,9} In the crystal structure of **H₂L¹**, the C–O bond length in the 2-hydroxy-3-methoxyphenyl part is shorter than the other (4-*tert*-butyl-2-hydroxyphenylimino part) {1.289(2) and 1.353(3) Å, respectively}. This difference between the C–O bond lengths is due to the keto structure being more dominant than the enol structure.

TABLE I. Crystal data and structure refinement parameters for **H₂L¹**

Empirical formula	C ₁₈ H ₂₁ NO ₃
Formula weight	299.36
Crystal system	Orthorhombic
Space group	<i>Pbca</i>
<i>a</i> (Å)	14.2349 (10)
<i>b</i> (Å)	9.5415 (5)
<i>c</i> (Å)	24.1061 (16)
α, β, γ (°)	90
<i>V</i> (Å ³)	3274.1(4)
<i>Z</i>	8
<i>D_c</i> (g cm ⁻³)	1.215
μ (mm ⁻¹)	0.082
θ range (°)	2.5–25.2
Measured refls.	46454
Independent refls.	3898
<i>R</i> _{int}	0.062
<i>S</i>	1.04
<i>R</i> 1/ <i>wR</i> 2	0.059/0.154
$\Delta\rho_{\max}/\Delta\rho_{\min}$ (eÅ ⁻³)	0.19/-0.21
CCDC	2298000

TABLE II. Hydrogen bonding parameters for **H₂L¹** (Å, °)

D–H···A	D–H	H···A	D···A	D–H···A
N1–H1···O1	0.88(2)	1.88(2)	2.598(2)	138(2)
O3–H3A···O1 ⁱ	0.83(2)	1.83(2)	2.657(2)	178(3)

Symmetry code: (i) $-x+1/2, y+1/2, z$.

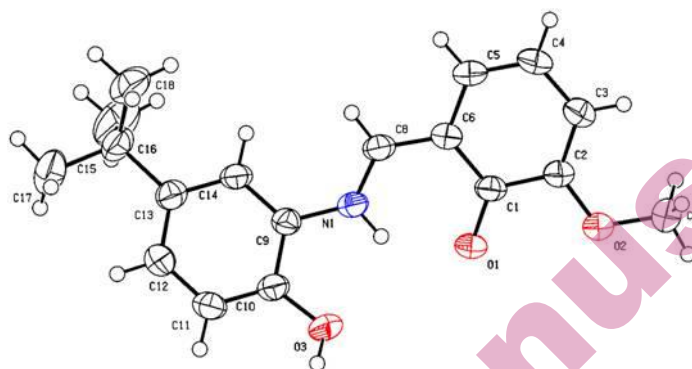


Fig. 2. Molecular structure of $\mathbf{H}_2\mathbf{L}^1$ showing the atom numbering scheme.

General properties

$\mathbf{H}_2\mathbf{L}^1$, an ONO type imine compound, is a dibasic and tridentate chelating ligand whereas \mathbf{HL}^2 is a monobasic bidentate chelating NO type ligand. ESI-MS data showing formation of the ligands are given in the experimental section, and the spectra are given as supplementary material (Figures S1 and S2). Both ligands appear to tend to form 1:1 complexes, which is probably due to the steric effect of the substituents which they have. It was also expected that \mathbf{HL}^2 , which is a bidentate ligand, would give a 1:2 complex, but the steric effect of the substituents and the character of the metal salt (chloride salts) can be considered as factors that favor the 1:1 formation.

The magnetic moment values of the Ni(II) complexes were found to be 2.04 and 2.05 BM for $\mathbf{H}_2\mathbf{L}^1$ and \mathbf{HL}^2 complexes, respectively. These values are lower than the 2.83 BM expected for octahedral or tetrahedral geometries, which are paramagnetic structures that the d^8 ion with two unpaired electrons may have. Such low values are generally thought to be due to the distorted geometry between the tetrahedral and square planar systems, called quasi-tetrahedral.⁴³⁻⁴⁵ Co(II) complex of $\mathbf{H}_2\mathbf{L}^1$ (**1a**) has a magnetic moment of 4.06 BM according to the measurements. It was reported that geometry of Co(II) complexes having magnetic moment values below 4.70 BM is trigonal bipyramide or square pyramidal (penta-coordinated).⁴⁶ According to this finding, the geometry of **1a** may be regarded as square pyramidal in a high-spin structure (three unpaired electrons). The magnetic moment value of Cu(II) complex of $\mathbf{H}_2\mathbf{L}^1$ (**1c**) at room temperature was found to be 1.72 BM, indicating formation of a monomeric Cu(II) complex. This value is very close to the theoretical value of 1.71 BM for the d^9 electron configuration. The Cu(II) complex of \mathbf{HL}^2 (**2c**) was found to be 1.01 BM, which indicates a Cu(II)-Cu(II) interaction. It is possible to suggest that a dimeric structure with a chloride bridge is formed in this complex and thus the Cu(II)-Cu(II) interaction occurs.

The magnetic moment value of the Co(II) complex of **HL**² (**2a**) was measured as 2.17 BM. This value indicates a structure with 1 and 2 unpaired electrons, which may result from a chloride-bridged structure or five-coordination geometry showing M-M interaction for the Co(II) ion with the *d*⁷ structure.⁴⁷

The molar conductivity values of the complexes except the Pd(II) complex of **H₂L**¹ (**1e**) in DMF were measured to be below 50 Ω⁻¹cm²mol⁻¹. According to Geary, compounds with a molar conductivity below 50 Ω⁻¹cm²mol⁻¹ are considered non-ionic or non-electrolyte.⁴⁸ It is possible to conclude that the Pd(II) complex of **H₂L**¹, which has a molar conductivity value of 83.2 Ω⁻¹cm²mol⁻¹, is 1:1 electrolyte. This result, which is also supported by the elemental analysis values, shows that the K[Pd(L¹)Cl] structure is possible.⁸

NMR spectra

NMR spectral data and their assignments of the ligands and the diamagnetic complexes are given in Experimental Section. ¹H- and ¹³C-NMR spectra of the compounds are given in Figures S3 – S14.

There is significant information for structural characterization of Schiff base **H₂L**¹ having two hydroxyl groups (salicylic and phenolic OHs) in the ¹H-NMR. The signals at 9.57 and 9.00 ppm should belong to phenolic OH and N=CH protons, respectively.¹⁰ Salicylic OH proton, on the other hand, was dissociated due to its high acidic character and its signal could not be detected by the device. As a result, it can be asserted that the keto state of **H₂L**¹ is dominant in the solid state while the enol state is dominant in the solution (Fig. 3). According to the crystal structure analysis, **H₂L**¹ has a keto structure in the solid state.

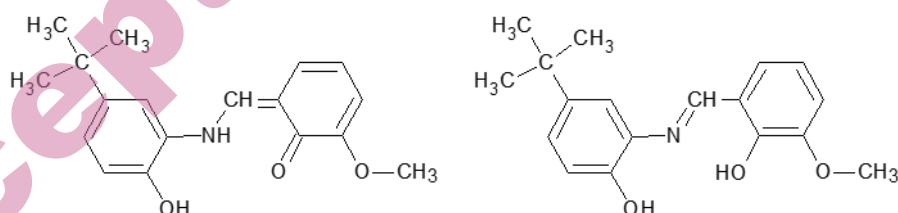


Fig. 3. Structure of **H₂L**¹ in solid state (keto form, left) and solution with polar solvents (enol form, right).

Phenolic protons of the ligands are not observed in the ¹H-NMR spectra of the Pd(II) and Zn(II) complexes, since they removed along with the complex formation. In addition, the azomethine proton (-N=CH-) of the Schiff base ligand is shifted to the lower frequency (upfield) on complexation, considerably. For example, N=CH proton shows shifting with 0.36 ppm (from 9.00 to 8.64 ppm) in the Pd(II) complex of **H₂L**¹. It appeared at 8.86 ppm in the Zn(II) complex.

The signal at 161.6 ppm in the ¹³C-NMR spectra of **H₂L**¹ should be due to azomethine carbon atom in enol form of the imine compound. The signals of the

carbon atoms bonded to the oxygen atom (C1, C2' and C3') of **H₂L¹** are detected at the 148.6 – 152.5 ppm range. In the Pd(II) complex, the azomethine carbon shifted to 174.3 ppm, while the carbon atoms to which the oxygen atoms are bonded were found to be between 161.5 and 146.9 ppm. In the Zn(II) complex, the N=CH carbon was detected at 164.8 ppm, while the carbon atoms bonded to oxygen were detected between 161.3 and 144.8 ppm.

In **HL²**, the NH and OH protons gave a single broad band at 13.12 ppm (integral value = 2H). The broad signals corresponding to a single proton seen at 13.64 and 13.22 ppm in the Zn(II) and Pd(II) complexes, respectively, should belong to the NH proton. The disappearance of the signal belonging to the OH proton indicates that this proton was removed with the complexation of the phenolic oxygen. Sufficient data could not be obtained from ¹³C-NMR analyses of complexes of **HL²**.

IR spectra

The major IR spectral data are presented in Experimental Section. FTIR spectra of the compounds are given as supplementary material (Figures S15 – S26). The IR spectra of the Schiff base (**H₂L¹**) and its complexes shows medium intensity absorption bands at 1630 – 1647 cm⁻¹ assigned to the $\nu(\text{C}=\text{N})$. The C=N stretching mode of the benzimidazolyphenol derivative (**HL²**) and its complexes are observed at the 1602 – 1619 cm⁻¹ range. The medium bands seen between 1576 and 1619 cm⁻¹ can be attributed to the C=C stretching mode of the ring systems, which is expected to appear around 1600 cm⁻¹. On complexation, considerable changes such as a shift to a higher wavenumber and a decrease in the intensity of absorptions were observed in the C=N band characteristic. These changes may support the argument the imine nitrogen atom coordination in the complexes of both Schiff base and benzimidazolyphenol ligands.

The strong bands at the 1182 – 1258 cm⁻¹ range are attributed to the C–O stretching vibrations of the ligands and the complexes.^{49,50}

In the spectra of all the compounds, generally weak bands appearing between 3054 and 3080 cm⁻¹ can be attributed to stretching vibration of aromatic CH; strong or medium intensity bands detected in the range of 812 – 831 cm⁻¹ can be interpreted as originating from the bending modes of aromatic CH groups.⁵¹

As a difference from the ligands, the new broad medium or weak bands between 667 cm⁻¹ and 688 cm⁻¹ in the IR spectra of the complexes, can be attributed to $\nu(\text{M} \leftarrow \text{N})$ coordination band (Fig. 4).²²

New medium bands at lower frequency at the 536 – 545 cm⁻¹ range in the complexes may be assigned to $\nu(\text{M} \leftarrow \text{OC})$ vibration frequencies and this finding can be considered as supported information for the phenolic oxygen atom coordination (Fig. 4).⁵²

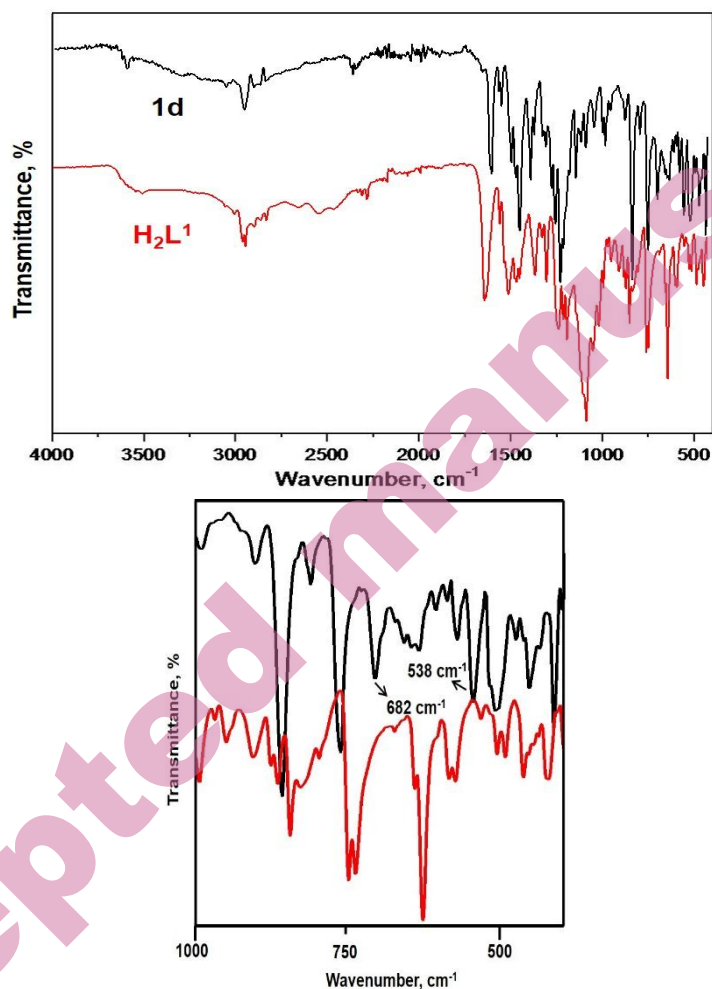


Fig. 4. Infrared spectra of $\mathbf{H_2L^1}$ and its Zn(II) complex ($\mathbf{1d}$).

UV-visible spectra

The UV-visible absorption spectra were obtained in dimethylsulfoxide (DMSO) at room temperature. Experimental maximum absorption wavelength data of the compounds are presented in Experimental section. UV-visible spectra of the compounds are given as supplementary material (Figures S27 – S38). The bands between 300 and 350 nm involve $\pi \rightarrow \pi^*$ transitions whereas the bands at the range of 350 – 400 nm can be attributed to $n \rightarrow \pi^*$ transitions. The band at 456 nm in $\mathbf{H_2L^1}$ is associated with intramolecular charge transfer transitions.⁵³

The absorptions at 451 and 458 nm in the Pd(II) complexes of $\mathbf{H_2L^1}$ and $\mathbf{HL^2}$, respectively, can be assigned to $d-d$ transitions and indicate square planar stereochemistry in solution and can be assigned to $^1A_{1g} \rightarrow ^1A_{2g}$ transition.⁹ The

weak bands appearing in the visible region can be attributed to *d-d* transitions. For example, the bands in the range of 433 – 478 nm in **1b**, **1c**, **2b** and **2c** {Ni(II) and Cu(II) complexes}, can be associated with the $^4A_2 \rightarrow ^4T_1(P)$ (ν_3) transition arising from a tetrahedral geometric structure.⁴² The 464 and 473 nm transitions observed in Co(II) complexes, for **1a** and **2a**, respectively, can be attributed to the $^3B(F) \rightarrow ^3E(P)$ transitions in the square pyramidal structure in solution environment.^{54,55} Since there are no allowed *d-d* transitions in Zn(II) complexes (**1d** and **2d**), the bands at the 350 – 465 nm range should originate from the intraligand and metal-to-ligand charge transfer transitions.

Fluorescence spectra

Fluorescence spectroscopy measurements of **HL**², a benzimidazolyphenol derivative, and its complexes were carried out. Fluorescence spectral data of the compounds, obtained at a concentration of approximately 1×10^{-4} mol/L in ethanol at room temperature, are given in experimental section (excitation wavelength: 354 nm). The fluorescence spectra of **HL**² and its complexes are given in Figure 5.

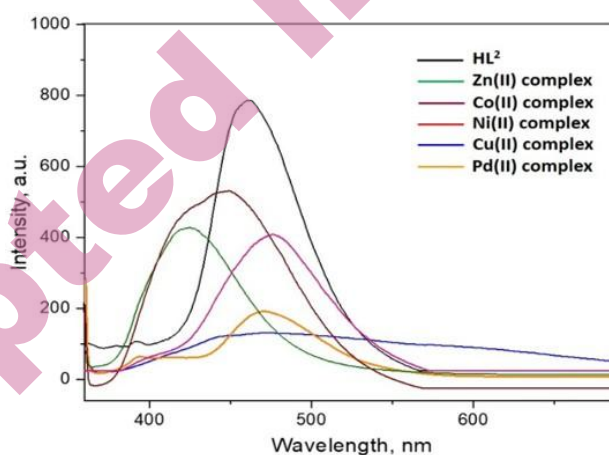


Fig. 5. Comparative fluorescence spectra of **HL**² and its complexes.

HL² emit at 463 nm strongly. In the complexes, the emission values vary between 425 and 478 nm and the intensity decreases. In Co(II), Cu(II) and Zn(II) complexes, emission is observed at a lower wavelength (blue shift) relative to the ligand, while in Ni(II) and Pd(II) complexes, it is observed at a higher wavelength (red shift). The common feature of the last two metal ions is that they both have the d^8 electronic configuration system. The fluorescence intensity decreases significantly in Pd(II) and Cu(II) complexes. This effect is particularly pronounced in the Cu(II) complex. This indicates that the Cu(II) ion quenches the fluorescence property of the ligand (quenching effect).

Thermogravimetric analysis

The weight loss data obtained from thermal analysis studies are outlined in Experimental. The samples were heated from room temperature up to 700 °C in air atmosphere. Thermogravimetric analysis (TGA) curves of complexes provide important clues for explaining the thermal behavior of molecules, and especially the state of water molecules. It is known that lattice H₂O molecules remove from the complex below 100 °C and coordinated H₂O molecules up to 200 °C. Approximately 9.5 and 12.3 % mass losses observed in TGA curves of Co(II) and Ni(II) complexes of **H₂L¹** (**1a** and **1b**), respectively, below 200 °C can be considered as an indication of presence of two moles of coordinated water molecules (Fig. 6). This valuation is reasonable, considering that two moles of H₂O in the complexes correspond to theoretical masses of 8.8 % and 9.2 %, respectively. The mass losses of 3.6 to 4.5 % observed in compounds **1a**, **1d**, **1e**, **2b**, and **2d** below 100 °C indicate the presence of one mole of lattice water in these compounds (The theoretical values for these complexes are at the 3.6 % – 4.5 % range). TGA curves of **2a** – **2e** are given as supplementary material in Figures S39 – S43.

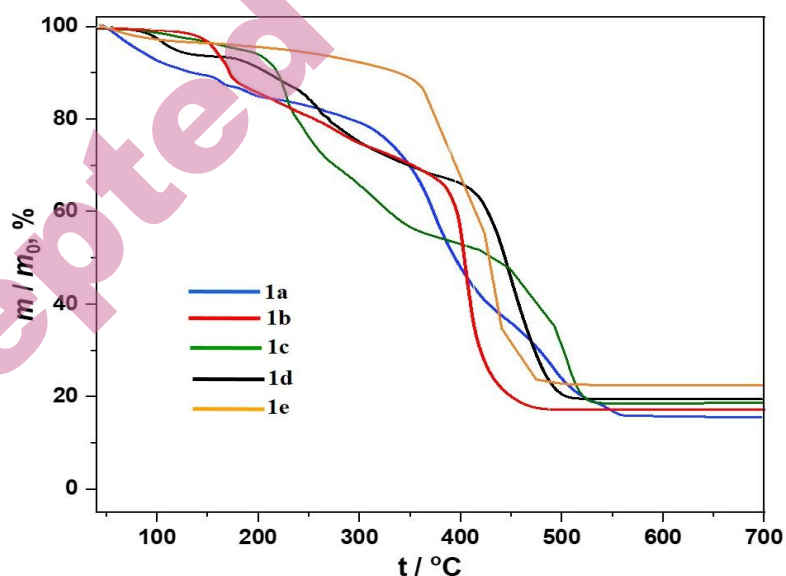


Fig. 6. TGA curves of the complexes **1a** – **1e**.

It was observed that the complexes began to decompose above 300 °C and completely decomposed above 500 °C, forming metal oxide forms. The mass ratios remaining from the complexes after complete decomposition are consistent with the theoretical mass ratios calculated for metal oxides.

Various complexes of H_2L^1 were reported in the literature. Griffiths *et al* reported the synthesis and crystal structure of heterobimetallic 3d/4f coordination cluster formulated as $[\text{Zn}_2\text{Y}_2(\text{L}^1)_4(\text{NO}_3)_2(\text{DMF})_2]$ and study its catalytic properties toward the Michael addition of nitrostyrenes with barbituric acid derivatives.²⁶ Effect of alcoholic solvent and acetate anion coordination mode variations on structures and magnetic properties of heterometallic Zn_2Dy_2 tetranuclear clusters was studied.^{27,28} Zhao *et al* reported tetranuclear complexes of H_2L^1 , $[\text{Ni}_4(\text{L}^1)_4(\text{CH}_3\text{OH})_4]$ and $[\text{Ni}_2\text{Zn}_2\text{Cl}_2(\text{L}^1)_2(\mu_{1,1}\text{-N}_3)_2]\cdot\text{H}_2\text{O}$, and investigated their antimicrobial activities.²⁹ All of these complexes have a tetranuclear structure. Some mononuclear diorganotin(V) complexes of H_2L^1 , R_2SnL^1 (R=Me, Et, Bu, Ph), were obtained and their antimalarial and antioxidant activities were investigated by Taxak *et al*.³⁰

Factors such as the crystallization method, the kind of metal salt used, and the solvent are effective in complex formation. In our study, we used chloride salts of metals and attempted to obtain single crystals using various solvents, but we were unsuccessful. Therefore, we do not have evidence to suggest that our complexes are mononuclear or polynuclear. It is also possible that some of our complexes are polynuclear or as in the literature. Consequently, in the light of the analytical and spectroscopic data obtained, the tentatively proposed structures in Figure 7 can be suggested for the complexes in the study.

Antimicrobial activity

In vitro antimicrobial activity test results of the ligands (H_2L^1 and HL^2) and their metal complexes in terms of MIC are presented in Table III in comparison with the values of the antibiotics and antifungal agents.

Table III shows that the benzimidazole derivative (HL^2) exhibits a higher antimicrobial effect compared to the Schiff base (H_2L^1), particularly against *S. epidermidis* (a Gram positive bacteria) and *C. tropicalis* (a fungi). On the other hand, it appears that the Co(II) complex of HL^2 (**2a**) has a potent activity against *S. aureus* and *E. coli*, the Ni(II) complex (**2b**) against both Gram positive bacteria (*S. aureus* and *S. epidermidis*), and the Cu(II) complex (**2c**) against *S. aureus*, *S. epidermidis* and *E. coli* compared to other complexes. Another noteworthy finding of the study was that **1a**, **1c**, **1d** and **1e** showed significantly higher activity against *C. tropicalis* compared to the ligand.

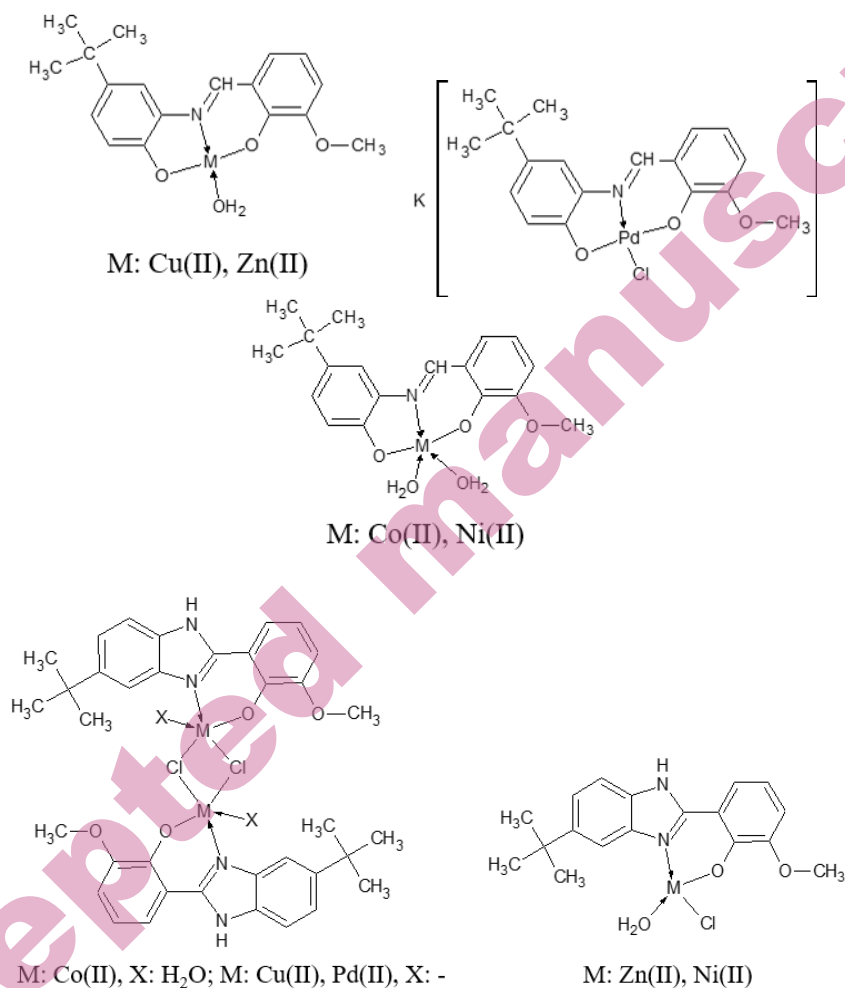


Fig. 7. Tentatively proposed structures for the complexes in the study.

In the literature, the antimicrobial activities of **H₂L¹** and its tetranuclear Ni(II) complex were investigated by Zhao *et al* against *S. aureus* and *E. coli* bacterial strains, which are also included in the bacterial group we studied.²⁹ They reported antimicrobial activities for **H₂L¹** of 75 μ M (*S. aureus*) and 37.5 μ M (*E. coli*), which differ greatly from our results (625 μ g/mL for both bacterial strains). There could be several reasons for such significantly different results in both studies. First, there is a difference in methods: The literature uses a colorimetric method using the dye MTT (3-(4,5-dimethylthiazol-2-yl)-2,5-diphenyltetrazolium bromide) published in 2000.⁵⁶ Our method is a relatively new method published by CLSI in 2021.³⁶ In addition, factors such as user errors and the chemicals used (DMSO,

culture medium, etc.) may also be influential. The reproducibility of the experiment is also important. Our experiments were repeated twice. The number of repetitions in the literature is not specified. Therefore, the difference in results can be considered reasonable.

TABLE III. *In vitro* antimicrobial activity of the compounds (MIC, $\mu\text{g/mL}$)

Compounds	Microorganisms								
	<i>Sa</i> ^a	<i>Se</i> ^a	<i>Ec</i> ^b	<i>Kp</i> ^b	<i>Pa</i> ^b	<i>Pm</i> ^b	<i>Ca</i>	<i>Cp</i>	<i>Ct</i>
H₂L¹	625	625	625	625	312	625	312	156	625
1a	312	312	625	625	625	625	312	-	156
1b	625	625	1250	625	-	625	1250	1250	312
1c	625	625	1250	1250	625	1250	625	625	156
1d	1250	156	1250	312	1250	625	1250	625	156
1e	312	625	312	625	625	625	312	156	156
HL²	625	156	312	-	625	625	-	1250	156
2a	78	156	78	156	312	312	312	625	156
2b	19.5	39	156	625	625	-	-	625	-
2c	78	19.5	78	312	625	-	625	625	312
2d	312	312	156	626	625	312	312	625	312
2e	312	312	312	312	625	-	-	312	-
Reference ^c	0.25	0.25	0.007	0.007	0.125	0.007	0.5	1.0	1.0

* *Sa* - *Staphylococcus aureus* ATCC 6538 ; *Se* / *Staphylococcus epidermidis* ATCC 12228 ; *Ec* - *Escherichia coli* ATCC 8739 ; *Kp* - *Klebsiella pneumoniae* ATCC 4352 ; *Pa* - *Pseudomonas aeruginosa* ATCC 1539 ; *Pm* - *Proteus mirabilis* ATCC 14153 ; *Ca* - *Candida albicans* ATCC 10231 ; *Cp* - *Candida parapsilosis* ATCC 22019 ; *Ct* - *Candida tropicalis* ATCC 750 ; ^a Gram positive ; ^b Gram negative ; - : No antimicrobial effect at 5000 $\mu\text{g/mL}$ and lower dilutions ; ^c: Ciprofloxacin and Amphotericin B were used for bacteria and fungi, respectively.

Antiviral activity

Antiviral activity of the compounds was tested against Parainfluenza Type-2 virus and the results are given at Table IV as percent inhibition. It was found that while **H₂L¹** inhibited viruses by 51 %, **HL²** was found to be effective with a rate of 26 %. Accordingly, it appears that Schiff base, **H₂L¹**, has approximately twice the antiviral effect than the benzimidazole compound, i.e. **HL²**.

In all complexes of **HL²**, the antiviral effect was significantly increased compared to the ligand. It is particularly interesting that **2a** and **2c** showed virus inhibition effect at the rates 62 % and 64 %, respectively (Fig. 8).

This study is limited to one Schiff base containing tert-butyl and methoxy groups, one benzimidazolylphenol ligand, and five complexes of each. More comprehensive studies can be conducted using a larger number of similar ligands and different complexes. For example, it might be interesting to investigate how the activities of compounds obtained by substituting the methoxy groups (e.g., 4- or 5-substituted) change. Changes in activity can be observed by forming complexes with different metal ions such as Mn(II), Fe(III), Ag(I), and VO(II).

One of the advantages of our study is that the activity against a wide range of bacteria and fungi has been investigated. Another advantage is that the antiviral effect has been investigated, and studies on the antiviral activity of such compounds are quite limited.

TABLE IV. Antiviral activity of the compounds

Compound	Virus Inhibition, %
H₂L¹	51
1a	37
1b	29
1c	34
1d	33
1e	42
HL²	26
2a	62
2b	52
2c	64
2d	43
2e	35
Ribavirin*	100

Ribavirin: Reference antiviral agent

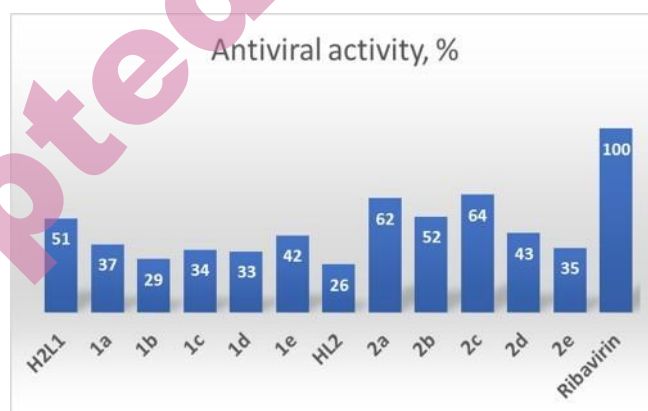


Fig. 8. Antiviral activity of the compounds in the study against Parainfluenza Type-2 virus

CONCLUSION

This study deals with two chelating ligands containing *tert*-butyl and methoxy groups in their structures, an ONO-type Schiff base (**H₂L¹**) and benzimidazolylpenol (**HL²**), an NO-type ligand, and their various transition metal complexes (**1a – 1e**, **2a – 2e**) and their various biological properties. A study group consisting of a total of 12 compound samples was formed by obtaining Co(II), Ni(II), Cu(II), Zn(II) and Pd(II) complexes of both ligands.

The structure of **H₂L¹** was investigated using single crystal X-ray diffraction spectroscopy. There is keto-enol tautomerism in **H₂L¹** according to spectral data. All the compounds were characterized by using physicochemical and spectroscopic methods such as elemental analysis, FT-IR, UV-vis and NMR spectroscopic techniques. Molar conductivity and magnetic moment measurements and thermogravimetric analysis were applied for the complexes also. Fluorescence spectroscopy was performed on **HL²** and its complexes due to their fluorescence properties.

In terms of biological applications, antibacterial, antifungal, and antiviral tests were performed on all compounds toward six bacteria, three fungi and Parainfluenza Type-2 virus. Generally, **HL²** and its complexes showed higher activity compared to **H₂L¹** and its complexes, especially on *S. aureus*, *S. epidermidis*, and *E. coli* bacteria, and the fungus *C. tropicalis*. Some of the complexes, such as **1a**, **1b**, and all complexes of **HL²**, shown higher activity than the ligands against many bacteria and *C. tropicalis*. In the comparison between the complexes, it was observed that **2a**, **2b**, and **2c** showed higher antibacterial activity, especially against *S. aureus*, *S. epidermidis*, and *E. coli*, compared to the others. Regarding antiviral activity, **H₂L¹** showed higher activity than **HL²** on Parainfluenza Type-2 virus. However, Co(II) and Cu(II) complexes of **HL²** (**2a** and **2c**) were observed to have the highest activity among the compounds, with rates of 62 % and 64 %, respectively.

SUPPLEMENTARY MATERIAL

Additional data are available electronically at the pages of journal website: <https://www.shd-pub.org.rs/index.php/JSCS/article/view/13789>, or from the corresponding author on request.

Acknowledgements: This work was supported by Scientific Research Projects Coordination Unit of Istanbul University-Cerrahpasa (Project number: 36370) and The Scientific and Technological Research Council of Türkiye (TUBITAK, Project number: 123Z795).

ИЗВОД

КОМПЛЕКСИ МЕТАЛА СА ШИФОВИМ БАЗАМА И БЕНЗИМИДАЗОЛИЛФЕНОЛНИМ ЛИГАНДИМА СА ТЕРЦ-БУТИЛ И МЕТОКСИ ГРУПАМА: СТРУКТУРНА КАРАКТЕРИЗАЦИЈА И БИОЛОШКО ИСПИТИВАЊЕ

DILDORA PARDAEVA¹, AYDIN TAVMAN^{2*}, MAYRAM HACIOGLU³, ONUR ŞAHİN⁴, MEHMET ALTUN⁵ И А. SEHER BIRTEKSÖZ TAN³

¹Istanbul University-Cerrahpaşa, Institute of Graduate Education, Department of Chemistry, 34320, Avcılar, Istanbul, Türkiye, ²Istanbul University-Cerrahpaşa, Faculty of Engineering, Department of Chemistry, Inorganic Chemistry Division, 34320, Avcılar, Istanbul, Türkiye, ³Istanbul University, Faculty of Pharmacy, Department of Pharmaceutical Microbiology, 34452, Beyazit, Istanbul, Türkiye, ⁴Sinop University, Faculty of Health Sciences, Department of Occupational Health and Safety, 57000 Sinop, Türkiye, and ⁵Istanbul University-Cerrahpaşa, Faculty of Engineering, Department of Chemistry, Organic Chemistry Division, 34320, Avcılar, Istanbul, Türkiye.

Синтетисана су и окарактерисана два хелатна лиганда са терц-бутил и метокси групама, Шифова база ОНО типа (H_2L^1) и бензимидазоллилфенолни дериват (HL^2), лиганд NO типа, као и њихови комплекси у реакцијама са CoCl_2 , NiCl_2 , CuCl_2 , ZnCl_2 и K_2PdCl_4 (**1a** – **1e**, **2a** – **2e**). За карактеризацију лиганда коришћене су различите физичкохемијске и спектроскопске технике. Поред тога, кристална структура H_2L^1 лиганда одређена је рендгенском структурном анализом. На основу спектроскопских података за H_2L^1 примећена је појава кето-енолне таутомерије. За карактеризацију комплекса коришћене су елементална анализа, моларна проводљивост, магнетна мерења, термогравиметријска анализа, FT-IR, флуоресцентна, UV-Vis и NMR спектроскопија (за дијамагнетне комплексе). Испитиване су антибактеријска, антигљивична и антивирусна активност синтетисаних једињења. Антимикробна активност једињења је испитивана према шест бактеријских и три гљивичне врсте. Неки од комплекса су показали већу активност према појединим микроорганизмима у односу на лиганде. Уочено је да HL^2 лиганд и његови комплекси показују већу активност у поређењу са H_2L^1 и његовим комплексима, нарочито према бактеријама *S. aureus*, *S. epidermidis* и *E. coli*, као и према гљивици *C. tropicalis*. Утврђено је да **2a** показује изражену активност према *S. aureus* и *E. coli*, **2b** према обе грам-позитивне бактерије (*S. aureus* и *S. epidermidis*), а **2c** према *S. aureus*, *S. epidermidis* и *E. coli* у поређењу са осталим комплексима. Антивирусна активност једињења испитивана је према вирусу параинфлуенце тип 2. У погледу антивирусног ефекта, H_2L^1 је показао већу активност од HL^2 , док су кобалт(II) и бакар(II) комплекси HL^2 лиганда показали највећу активност међу свим једињењима, са процентима инхибиције од 62% и 64%, редом.

(Примљено 17. фебруара; ревидирано 27. фебруара; прихваћено 2. јуна 2026.)

REFERENCES

1. A. Çınarlı, D. Gürbüz, A. Tavman, A. S. Birteksöz, *Chinese J. Chem.* **30** (2012) 449 (<https://doi.org/10.1002/cjoc.201180473>)
2. D. Gürbüz, A. Çınarlı, A. Tavman, A. S. Birteksöz, *Chinese J. Chem.* **30** (2012) 970 (<https://doi.org/10.1002/cjoc.201100237>)
3. B. S. Kusmariya, A. P. Mishra, *J. Mol. Struct.* **1130** (2017) 727. (<https://doi.org/10.1016/j.molstruc.2016.11.009>)
4. D. Gürbüz, A. Çınarlı, A. Tavman, A. S. B. Tan, *Bull. Chem. Soc. Ethiop.* **29** (2015) 63. (<https://doi.org/10.4314/bcse.v29i1.6>)

5. E. Alterhoni, A. Tavman, D. Gürbüz, M. Hacıoğlu, A. Çınarlı, O. Şahin, A. S. B. Tan, *ChemistrySelect* **5** (2020) 9730 (<https://doi.org/10.1002/slct.202001498>)
6. R. Y. Sumaiya, S. A. Chhanda, A. Wasif, F. Zohora, K. Akhter, M. S. Islam, N. Uddin, M. E. Halim, *J. Mol. Struct.* **1355** (2026) 145000 (<https://doi.org/10.1016/j.molstruc.2025.145000>)
7. G. Yenişehirli, N. A. Öztaş, E. Şahin, M. Çelebier, N. Ancın, S. G. Öztaş, *Heteroat. Chem.* **21** (2010) 373 (<https://doi.org/10.1002/hc.20628>)
8. D. Pardaeva, A. Tavman, D. Gürbüz, M. Hacıoğlu, F. N. Yılmaz, O. Şahin, A.S. B. Tan, A. Çınarlı, *Rev. Roum. Chim.* **69** (2024) 83 (<https://doi.org/10.33224/rch.2024.69.1-2.10>)
9. D. Pardaeva, A. Tavman, E. Erçağ, M. Hacıoğlu, D. Gürbüz, A. Çınarlı, A.S. Birteksöz Tan, *Fr. Ukr. J. Chem.* **12** (2024) 92. (<https://doi.org/10.17721/fujcV12IIP92-110>)
10. E. Alterhoni, A. Tavman, M. Hacıoğlu, O. Şahin, A. S. B. Tan, *J. Mol. Struct.* **1229** (2021) 129498 (<https://doi.org/10.1016/j.molstruc.2020.129498>)
11. S. Y. Ebrahimipour, I. Sheikhshoae, A. C. Kautz, M. Ameri, H. Pasban-Aliabadi, H. A. Rudbari, G. Bruno, C. Janiak, *Polyhedron* **93** (2015) 99 (<https://doi.org/10.1016/j.poly.2015.03.037>)
12. L. A. Alfonso-Herrera, S. Rosete-Luna, D. Hernández-Romero, J. M. Rivera-Villanueva, J. L. Olivares-Romero, J. A. Cruz-Navarro, A. Soto-Contreras, A. Arenaza-Corona, D. Morales-Morales, R. Colorado-Peralta, *ChemMedChem* **17** (2022) e202200367 (<https://doi.org/10.1002/cmdc.202200367>)
13. Z.-J. Zhang, H.-T. Zeng, Y. Liu, D.-Z. Kuang, F.-X. Zhang, Y.-X. Tan, W.-J. Jiang, *Inorg. Nano-Metal Chem.* **48** (2018) 486. (<https://doi.org/10.1080/24701556.2019.1571513>)
14. G. Sahu, E. R. Tiekink, R. Dinda, *Inorganics*, **9** (2021) 66 (<https://doi.org/10.3390/inorganics9090066>)
15. N. Patel, A. K. Prajapati, R. N. Jadeja, R. N. Patel, S. K. Patel, I. P. Tripathi, N. Dwivedi, V. K. Gupta, R. J. Butcher, *Polyhedron* **180** (2020) 114434. (<https://doi.org/10.1016/j.poly.2020.114434>)
16. Y. Ma, H. Liu, C. Li, Y. Zhang, M. Lv, D. Mu, S. Yin, R. Liu, *J. Mol. Struct.* **1309** (2024) 138172 (<https://doi.org/10.1016/j.molstruc.2024.138172>)
17. W. Y. Zhu, K. Liu, X. Zhang, *Sens. Diagn.* **2** (2023) 665 (<https://doi.org/10.1039/d3sd00020f>)
18. R. Sathyanarayana, V. Kumar, G.H. Pujar, B. Poojary, M.K. Shankar, S. Yallappa, *J. Photochem. Photobiol. A: Chem.* **401** (2020) 112751 (<https://doi.org/10.1016/j.jphotochem.2020.112751>)
19. A. Tavman, M. Hacıoğlu, D. Gürbüz, A. Cınarlı, M. A. F. Oksüzömer, A. S. B. Tan, *Bull. Chem. Soc. Ethiop.* **33** (2019) 451 (<https://doi.org/10.4314/bcse.v33i3.6>)
20. A. Tavman, A. Cınarlı, D. Gürbüz, A.S. Birteksöz, *J. Iran. Chem. Soc.* **9** (2012) 815 (<https://doi.org/10.1007/s13738-012-0098-z>)
21. A. Tavman, D. Gürbüz, A. A. Karaçelik, D. N. Çolak, D. Efe, A. Cınarlı, *Rev. Roum. Chim.* **69** (2024) 201 (<https://doi.org/10.33224/rch.2023.68.10-12.07>)
22. A. Tavman, A. Z. Elmal, D. Gürbüz, M. Hacıoğlu, A.S. Birteksöz Tan, A. Çınarlı, *Rev. Roum. Chim.* **68** (2023) 49 (<https://doi.org/10.33224/rch.2023.68.1-2.05>)
23. A. Tavman, D. Gürbüz, Ş. Öksüz, A. Çınarlı, *Mor. J. Chem.* **6** (2018) 328 (<https://revues.imist.ma/index.php/morjchem/article/view/7909/6695>)

24. X. Totta, A. A. Papadopoulou, A. G. Hatzidimitriou, A. Papadopoulos, G. Psomas, *J. Inorg. Biochem.* **145** (2015) 79 (<https://doi.org/10.1016/j.jinorgbio.2015.01.009>)
25. A. Kerflani, K. S. Larbi, A. Rabahi, A. Bouchoucha, S. Zaater, S. Terrachet-Bouaziz, *Inorg. Chim. Acta* **529** (2022) 120659 (<https://doi.org/10.1016/j.ica.2021.120659>)
26. K. Griffiths, A. Tsipis, P. Kumar, O. P. E. Townrow, A. Abdul-Sada, G. R. Akién, A. Baldansuren, A. C. Spivey, G. E. Kostakis, *Inorg. Chem.* **56** (2017) 9563 (<https://doi.org/10.1021/acs.inorgchem.7b01011>)
27. H. Ke, W. Wei, Y.-Q. Zhang, J. Zhang, G. Xie, C. Gang, S. Chen, *Dalton Trans.* **47** (2018) 16616 (<http://dx.doi.org/10.1039/C8DT03983F>)
28. H. Ke, W. Wei, Y. Yang, J. Zhang, Y.-Q. Zhang, G. Xie, S. Chen, *Dalton Trans.* **48** (2019) 7844 (<https://doi.org/10.1039/C9DT01074B>)
29. J. Zhao, J. Ji, S. Wang, Y. Luo, Z. You, *J. Coord. Chem.* **74** (2021) 3127 (<https://doi.org/10.1080/00958972.2021.2024522>)
30. B. Taxak, J. Devi, B. Kumar, M. Rani, *J. Mol. Struct.* **1322** (2025) 140309 (<https://doi.org/10.1016/j.molstruc.2024.140309>)
31. Chemazone online chemical service of Aurora fine chemicals
<https://chemazone.com/info?ID=136.567.528> (27 March 2026)
32. H. F. Ridley, G. W. Spickett, G. M. Timmis, *J. Het. Chem.* **2** (1965) 453 (<https://doi.org/10.1002/jhet.5570020424>)
33. Z. Karimi-Jaberi, M. Amir, *E-J. Chem.* **9** (2012) 167 (<https://doi.org/10.1155/2012/793978>)
34. O. S. Ürgüt, A. Tavman, M. G. Eser, *Chem. J. Mold.* **17** (2022) 73 (<http://dx.doi.org/10.19261/cjm.2022.957>)
35. M27-A3: *Clinical and Laboratory Standards Institute (CLSI), Reference Method for Broth Dilution Antifungal Susceptibility Testing of Yeasts*; Approved Standard-Third Edition (2012)
36. M100-Ed.31: *Clinical and Laboratory Standards Institute (CLSI), Performance Standards for Antimicrobial Susceptibility Testing* (2021)
37. K. Fukushima, T. Takahashi, M. Takaguchi, H. Ueyama, S. Ito, Y. Kurebayashi, T. Kawanishi, J. L. McKimm-Breschkin, T. Takimoto, A. Minami, T. Suzuki. *Biol. Pharm. Bull.* **34** (2011) 996 (<https://doi.org/10.1248/bpb.34.996>)
38. G. M. Sheldrick, *Acta Cryst.* **A64** (2008) 112 (<https://doi.org/10.1107/S0108767307043930>)
39. G. M. Sheldrick, *Acta Cryst.* **C71** (2015) 3 (<https://doi.org/10.1107/S2053229614024218>)
40. APEX2: Bruker AXS Inc. Madison Wisconsin USA (2013)
41. C. F. Macrae, I. J. Bruno, J. A. Chisholm, P. R. Edgington, P. McCabe, E. Pidcock, L. Rodriguez-Monge, R. Taylor, J. van de Streek, P. A. Wood, *J. Appl. Cryst.* **41** (2008) 466 (<https://doi.org/10.1107/S0021889807067908>)
42. L. J. Farrugia, *J. Appl. Cryst.* **45** (2012) 849 (<https://doi.org/10.1107/S0021889812029111>)
43. D. Lomjanský, C. Rajnák, J. Titis, J. Monco, L. Smolko, R. Boča, *Inorg. Chim. Acta* **483** (2018) 352 (<https://doi.org/10.1016/j.ica.2018.08.029>)
44. A. G. Starikov, R. M. Minyaev, V. I. Minkin, *Chem. Phys. Lett.* **459** (2008) 27 (<https://doi.org/10.1016/j.cplett.2008.04.132>)
45. A. J. Bridgeman, *Dalton Trans.* **2008** (2008) 1989 (<https://doi.org/10.1039/B717767D>)

46. E. Kwaskowska-Chec, M. Kubiak, T. Glowiak, J.J. Ziolkowski, *Transit. Met. Chem.* **23** (1998) 641 (<https://doi.org/10.1023/A:1006909528805>)
47. D. L. Reger, A. E. Pascui, E. A. Foley, M. D. Smith, J. Jezierska, A. Wojciechowska, S. A. Stoian, A. Ozarowski, *Inorg. Chem.* **56** (2017) 2884 (<https://doi.org/10.1021/acs.inorgchem.6b02933>)
48. W. Geary, *Coord. Chem. Rev.* **7** (1971) 81 ([https://doi.org/10.1016/S0010-8545\(00\)80009-0](https://doi.org/10.1016/S0010-8545(00)80009-0))
49. R. Singh, A. Prakash, S. K. Dhiman, B. Balagurumurthy, A. K. Arora, S. K. Puri, T. Bhaskar, *Bioresour. Technol.* **165** (2014) 319 (<https://doi.org/10.1016/j.biortech.2014.02.076>)
50. E. Kaki, A. Altindal, B. Salih, Ö. Bekaroglu, *Dalton Trans.* **44** (2015) 8293 (<https://doi.org/10.1039/C5DT00540J>)
51. L. J. Duarte, R. E. Bruns, *J. Phys. Chem. A* **122** (2018) 9833 (<https://doi.org/10.1021/acs.jpca.8b09141>)
52. K. I. Hadjiivanov, D. A. Panayotov, M. Y. Mihaylov, E. Z. Ivanova, K. K. Chakarova, S. M. Andonova, N. L. Drechev, *Chem. Rev.* **121** (2021) 1286 (<https://doi.org/10.1021/acs.chemrev.0c00487>)
53. Y. Kaya, H. Mutlu, G. Irez, *Gazi Univ. J. Sci.* **23** (2010) 13 (<https://dergipark.org.tr/en/download/article-file/82956>)
54. H. G. Bheemanna, V. Gayathri, N. M. N. Gowda, *IOSR-J. App. Chem.* **7** (2014) 17 (<https://doi.org/10.9790/5736-07421722>)
55. S. Tripathi, A. Dey, M. Shanmugam, R. S. Narayanan, V. Chandrasekhar, *Cobalt(II) Complexes as Single-Ion Magnets*, in *Organometallic Magnets. Topics in Organometallic Chemistry*, V. Chandrasekhar, F. Pointillart (eds), Springer, Cham, 2018 (https://doi.org/10.1007/3418_2018_8).
56. J. Meletiadis, J.F. Meis, J.W. Mouton, J.P. Donnelly, P.E. Verweij, *J. Clin. Microbiol.*, **38** (2000) 2949 (<https://doi.org/10.1128/jcm.38.8.2949-2954.2000>).